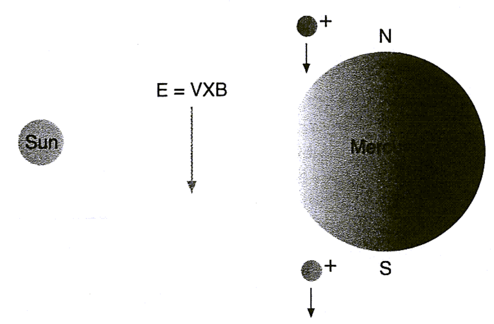

Figure 6.5. Na^+ and K^+ will interact in the electric fields in and around Mercury's magnetosphere and the IMF. Such ions will eventually be swept away into the interplanetary medium or will impact on Mercury's surface, become neutralized and eventually be recycled to the atmosphere unless they find a permanent cold trap. Mercury's magnetic field is not considered in the diagram. See text for explanation of E, V, and B.

composition reflect, in a significant way, the surface composition? It is of great importance to know if Mercury has more Na and K than is expected from our understanding of how planets form. Also important is whether Mercury ever had water, and if so how much? The study of the exosphere may help us answer these questions.

7

General surface features and radar characteristics

7.1 IMAGING MERCURY

Mariner 10 photographed only about 45% of Mercury's surface. The image resolution ranges from about 2 km down to 100 m at a few locations. Images revealed a heavily cratered and wrinkled terrain with no obvious signs of volcanic constructs or plate tectonics. The first glimpse of the images was tremendously exciting because no detailed ground-based images of the planet existed, and maps and drawings were lacking in detail, and seldom agreed on what detail they did exhibit. The generalized statement was "Mercury looks a lot like the Moon." In fact, this generalized impression has lingered in the minds of people although new and surprising ground-based observations show it to be unlike the Moon in several important ways. The internal characteristics are totally unlike the Moon.

7.1.1 Photomosaics of one hemisphere

As *Mariner 10* approached Mercury on its first encounter, it imaged the half-lit hemisphere centered on the prime meridian, 0° longitude. As it departed, *Mariner 10* imaged the opposite half-lit hemisphere centered on the 180° meridian (Figure 7.1). On the second encounter, the spacecraft imaged the south polar region, joining the two sides previously imaged on the first encounter. On the third encounter *Mariner 10* concentrated on taking high-resolution images of the two hemispheres imaged on the first encounter. Unfortunately, by this time the tape recorder had failed and the spacecraft was so far from Earth that the signal was very weak. Full frame real time images would have been so noisy that they would have been of little use. Therefore, only $\frac{1}{4}$ frame images were transmitted. Although almost all of the hemisphere between 10 and 180° was imaged, much of it was seen at very at high Sun angles where terrain analysis is difficult to impossible. As a consequence only about 25% of the planet was viewed at Sun angles that were favorable to geologic studies.

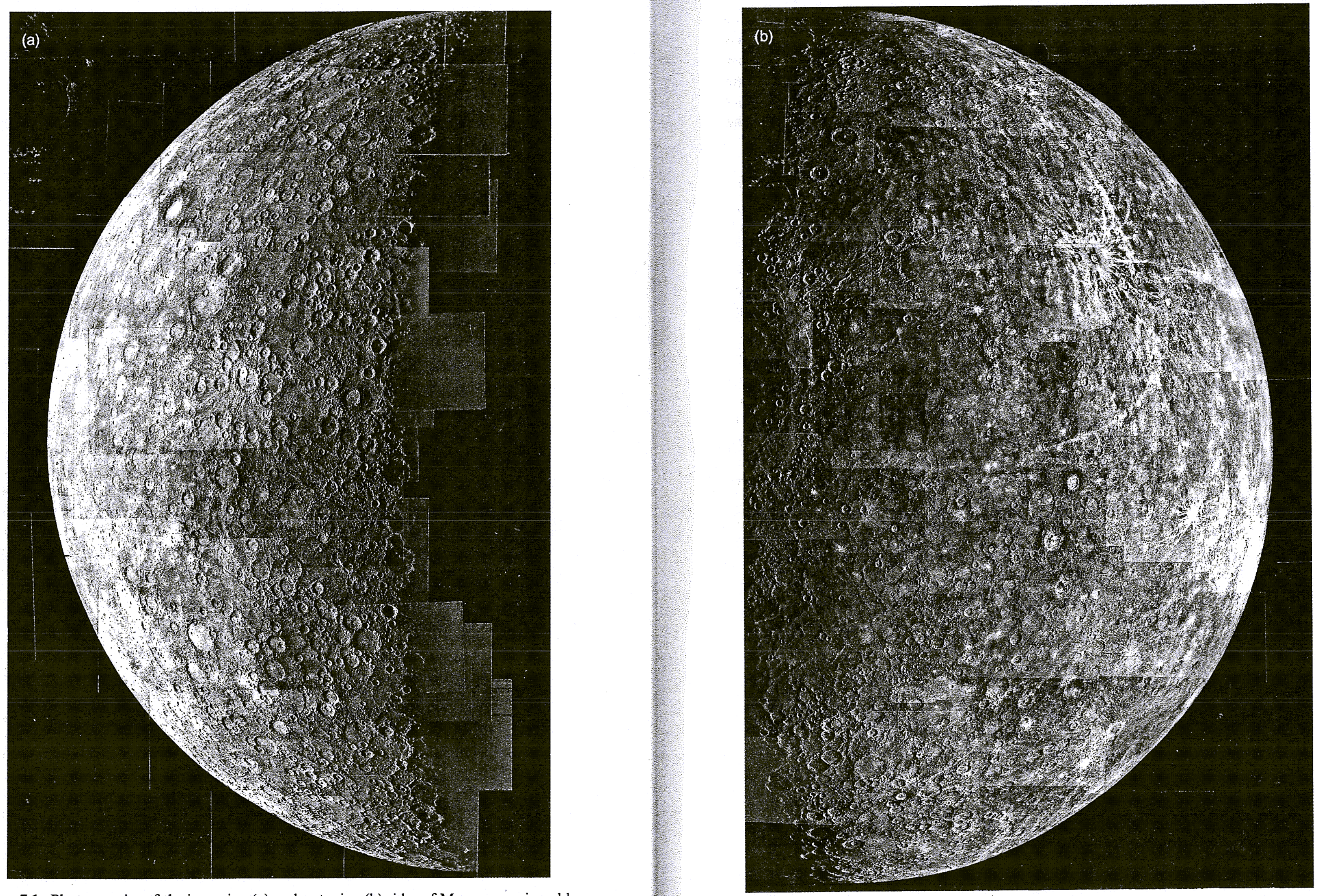

Figure 7.1. Photomosaics of the incoming (a) and outgoing (b) sides of Mercury as viewed by *Mariner 10*. Most of the smooth plains are concentrated on the outgoing side.

Whether or not the major features seen on this part of Mercury are representative of the planet as a whole is not known and must await further exploration. The first two flybys imaged almost all of the hemisphere between 10 and 190° longitude. Only about 5% of the northern part of this hemisphere was not imaged. Part of the same surface imaged at different viewing angles between the first and second encounters provided some stereo coverage which was useful in geologically mapping the surface.

7.2 MAJOR SURFACE FEATURES

The *Mariner 10* images revealed a heavily cratered planet with some large patches of smooth plains. There were also sinuous ridges and a peculiar broken-up terrain on the incoming side. The largest feature viewed by *Mariner 10* was the half illuminated Caloris basin. This basin is about 1300 km in diameter and has a peculiar fractured and ridged floor. In general, Mercury looked similar to the Moon (Figure 7.1).

7.2.1 Just another moon?

Up to this point it may seem that Mercury and the Moon have a lot in common. Some major differences and similarities have been pointed out, but many people look at Mercury and see it as the Moon's twin with a similar history. This perception could not be farther from the truth. Mercury is distinctly different from the Moon in many fundamental ways. Its similarities, although important, are few compared to its differences (Table 7.1).

The main similarity between Mercury and the Moon is that both display heavily cratered highlands that are the result of the period of late heavy bombard-

Table 7.1. Comparisons between Mercury and the Moon.

Similarities to the Moon
Heavily cratered surface
Smooth plains associated with impact craters and basins
Regolith (impact produced surface layer)
Differences from the Moon
Large iron core ~75% of the diameter
Relatively strong magnetic field
Exosphere dominated by sodium (Na) and potassium (K)
Large areas of intercrater plains (the major terrain type)
Comparable geologic units are brighter
Widespread distribution of thrust faults
Unique impact basin floor structure (Caloris basin)
Unique radar feature
Very strong radar backscatter from polar deposits
Origin

ment which ended about 3.8 billion years ago. Both bodies also have a regolith that was generated by the continuous rain of particles of all sizes onto the surface. This would also be true of any other bodies that did not have appreciable atmospheres or weathering processes. For example, asteroids and the small moons of Mars also have regoliths. Another similarity between the Moon and Mercury are the large areas of smooth plains associated with impact basins. Although both of these deposits may be lava, the compositions may be significantly different.

7.2.2 Mercury is unique

The differences from the Moon are many and significant. Mercury has the largest iron core (~75% of its radius) compared with its size of any planet or satellite in the Solar System. Although the Moon may have an iron core it is very small compared with other planets and satellites. Mercury is the only terrestrial planet other than Earth that has a dipole magnetic field or a very strong remanent field. The Moon has none at the present time, although it may have small areas of remanent magnetization. Mercury has large areas of intercrater plains in the highlands. In fact, they are the major terrain type on the part of Mercury imaged by *Mariner 10*. Although the Moon does have some patches of intercrater plains they are extremely small (~6% of the surface) compared with those on Mercury (~45%). Mercury displays a widespread, possibly global, distribution of thrust faults that form a unique tectonic framework unlike any other planet or satellite. The basin floor structure of the Caloris basin is unique and has no counterpart elsewhere in the Solar System. The smooth plains and other geologic units have higher albedos than comparable units on the Moon. This may indicate significant differences in composition. Unlike the Moon, Mercury displays strong radar-backscattering patches in the permanently shaded areas of the polar regions. Also, unlike the Moon, there is a large unique radar feature (Feature C) that has no counterpart elsewhere in the Solar System. Finally, the origin of Mercury must be totally different from the Moon. The Moon was probably formed as a result of a large planet-sized impact with the Earth near the end of the final accretion of the planets. This is obviously not the case for Mercury. In fact, the origin of Mercury's enormous iron core requires an origin far different from that of the Moon.

These great contrasts in characteristics between the Moon and Mercury require different processes and/or intensities for shaping the two bodies. Furthermore, their histories must be quite disparate in order to explain these differences. Although comparisons between the Moon and Mercury can be useful, one must use extreme caution in taking these comparisons too far when considering their histories.

7.3 MAPPING MERCURY

7.3.1 The coordinate system

All maps require a coordinate system consisting of latitudes and longitudes by which features are located. The location of the prime meridian (0°) is completely arbitrary.

On Earth, the prime meridian passes through the Greenwich Observatory on the outskirts of London, because it was here that most of the observations required to define longitudes had been made. Only on Earth and the Moon are the longitudes measured 180° east and west of the prime meridian. On all other planets and satellites longitudes are measured 360° east or west of the prime meridian.

The prime meridian on Mercury was selected to pass through the subsolar point when the planet is at perihelion. Because of Mercury's 3:2 resonance between its orbital and rotational period, one hemisphere faces the Sun at one perihelion passage, and the other hemisphere faces the Sun at the next perihelion passage. Consequently, there are two perihelion subsolar points 180° apart. To resolve this ambiguity, the International Astronomical Union in 1970 defined the prime meridian to pass through the subsolar point at the first perihelion after 1 January, 1950.

Mariner 10 did not see the area containing the prime meridian because it was 10° into the night side during the three encounters. However, the center of a small, well-defined crater observed on one of the high-resolution images was calculated to lie within 0.5° of the 20° meridian as defined by the International Astronomical Union's perihelion convention. It was decided that the center of this crater would exactly coincide with the 20° meridian, and to serve as a reference for locating all other longitudes. This 1.5 km diameter crater was called Hun Kal – the number 20 in the ancient Mayan language (Figure 7.2). The Mayans were the most advanced

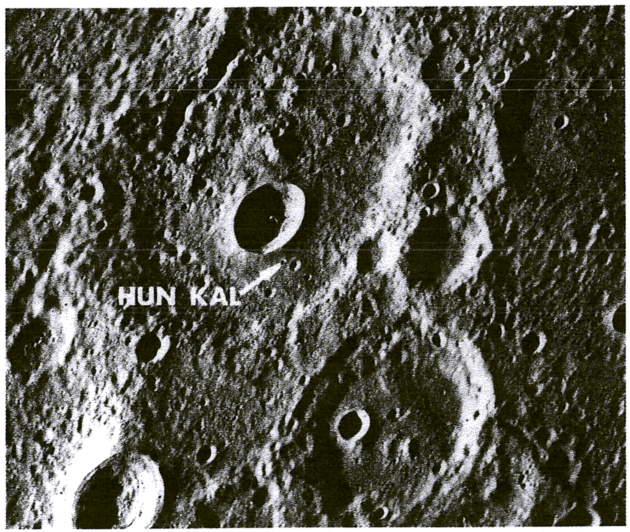

Figure 7.2. This high resolution *Mariner 10* image shows the position of the small crater Hun Kal (1.5 km diameter), which was used to define the 20° meridian on Mercury.

astronomers in the ancient Americas and used a numbering system based on twenty, rather than the base 10 used in Western civilization. The coordinates of many features were determined from the spacecraft *Ephemeris* (spacecraft position at various times). These were then used to position the latitude–longitude grid with respect to the topography. Longitudes were measured from 0 to 360° increasing to the west. Recent high-resolution radar images of the polar regions have been used to position this latitude–longitude grid much more accurately. These observations show that the pole position is inacurate by 65 ± 2 km from the position shown on the current maps. The new pole position is accurate to 0.05°. The coordinate system on current maps needs to be adjusted by 65 kms.

7.3.2 Naming features on Mercury

The surface of Mercury is divided into 15 areas called quadrangles. Figure 7.3 shows the position of the quadrangles used to identify regions of Mercury. Each map is designated by the letter H (for Hermes, the Greek equivalent of Mercury) followed by a number from 1 to 15. Nine of these quadrangles viewed by *Mariner 10* have been compiled into shaded relief maps at a scale of 1:5 million. Unfortunately large parts of three of these quadrangles were not imaged by *Mariner 10* so they are very incomplete. The nine quadrangles are further designated by the names of prominent surface features contained in the areas. For example, the south polar map is called the Bach (H-15) quadrangle since there is a large crater in the area by that name.

Craters on Mercury are named after famous people in the arts, including artists, authors, and musicians, such as Dickens, Michelangelo, and Beethoven. There are, however, exceptions. The crater Hun Kal is named after the number 20 in the Mayan language as explained earlier. Also the bright rayed crater Kuiper is named after a famous astronomer who was a member of the *Mariner 10* science team before his untimely death in December 1973. Prominent ridges or scarps (called "rupes" from Latin) are usually named after ships of exploration and scientific research, such as *Discovery* and *Victoria.* Exceptions are two prominent ridges named Antoniadi and Schiaparelli for the astronomers who first mapped Mercury from Earth-based observations. Valleys (called "valles" from Latin) are named after prominent radio observatories such as Arecibo and Goldstone. Plains (called "planitiae" from Latin) are named after the word for the planet Mercury in various languages, and for gods from ancient cultures who had a role similar to that of the Roman god Mercury. Typical names are Odin (Scandinavian) and Tir (Germanic). Borealis Planitia (Northern Plains) and Caloris Planitia (Plains of Heat) are exceptions.

7.3.3 Maps and topographic representations

There have been a number of maps prepared from the imaging data. The map shown in Figure 7.4 is a shaded relief map of Mercury's Shakespeare quadrangle. This type of map is prepared by highly trained artists using airbrushes.

An *Atlas of Mercury* was compiled from *Mariner 10* images and is the most comprehensive set of maps of the *Mariner 10* coverage. The atlas consists of

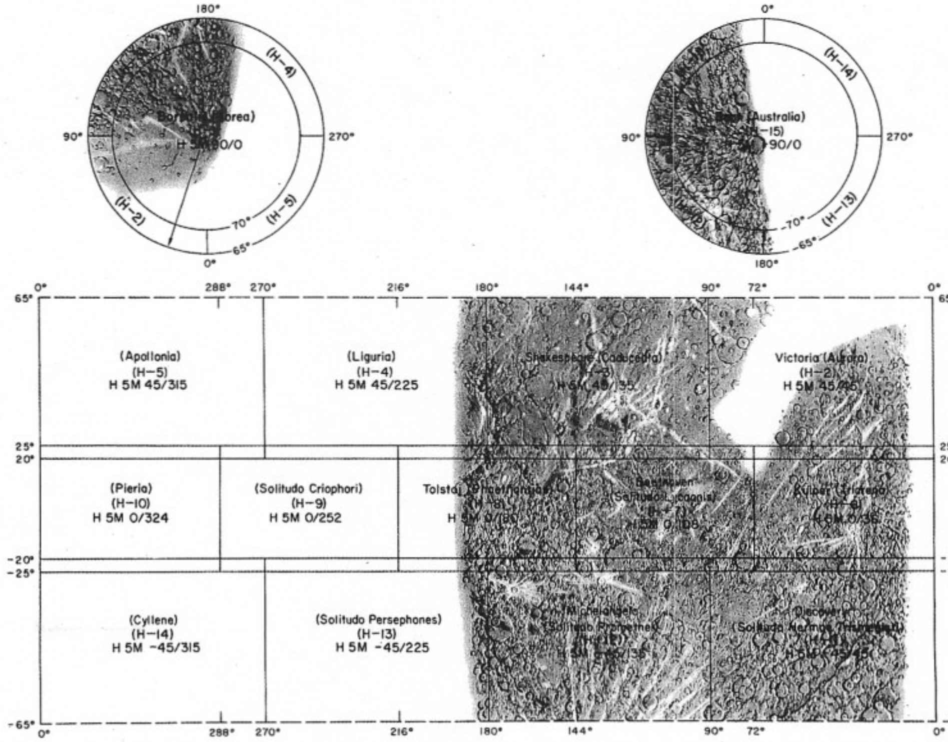

Figure 7.3. This map shows the distribution and names of the 15 (1:5 million scale) quadrangles (also on the CD). Only nine of these quadrangles were wholly or partly imaged by *Mariner 10*. About 55% of the planet remains unexplored (from Atlas of Mercury).

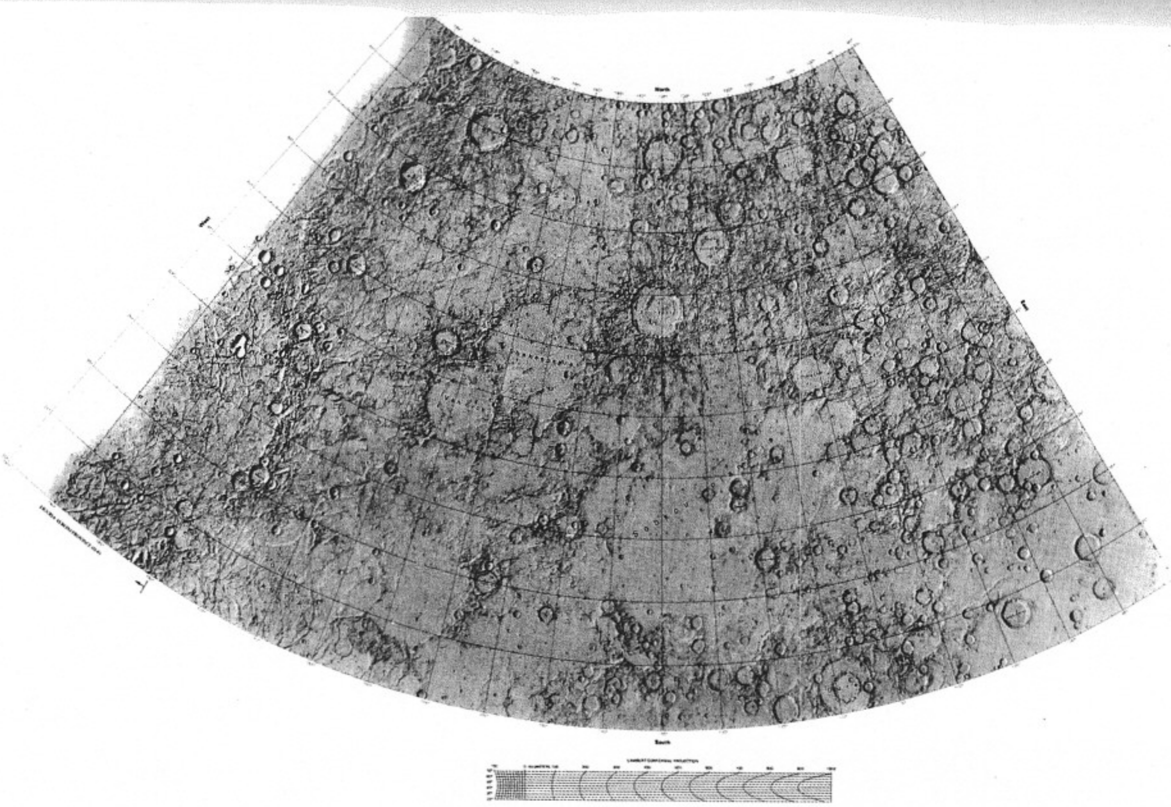

Figure 7.4. A US Geological Survey shaded relief map of Mercury's Shakespeare quadrangle (H-3) (from Atlas of Mercury and on the CD).

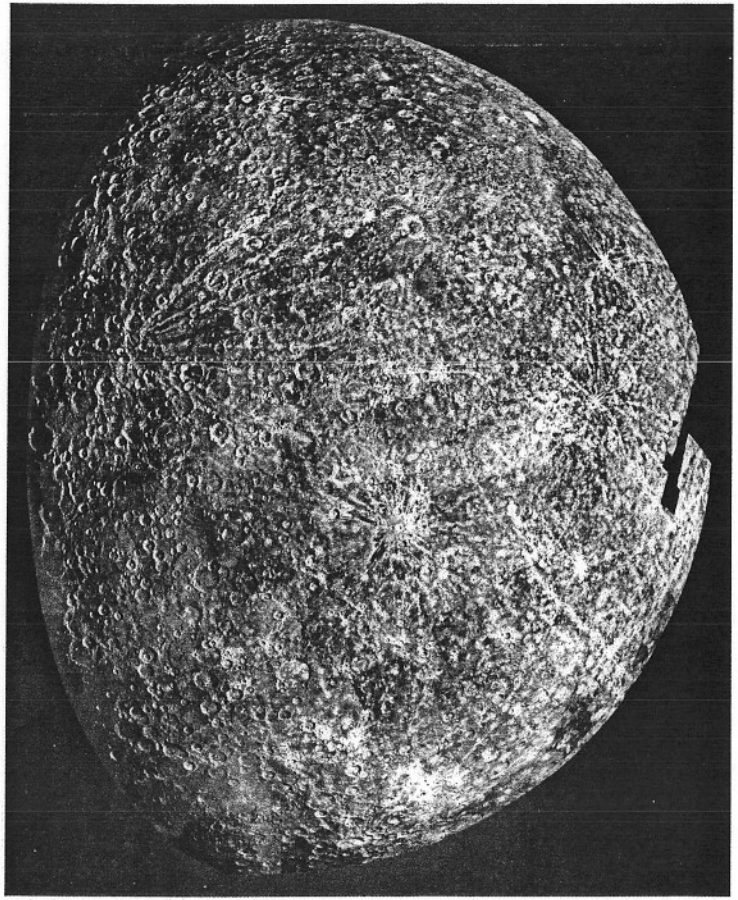

Figure 7.5. Photomosaic of Mercury's south polar region, taken by *Mariner 10* on its second encounter.

photomosaics and shaded relief maps of each quadrangle plus individual images of interesting features. It also includes some stereo images acquired from the first and second encounters. Figure 7.5 shows one of the photomosaics from this atlas, and Figure 7.6 is a photomosaic of the entire equatorial region. The accompanying CD contains all of the photomosaics, airbrush maps, and the best single images from *Mariner 10*.

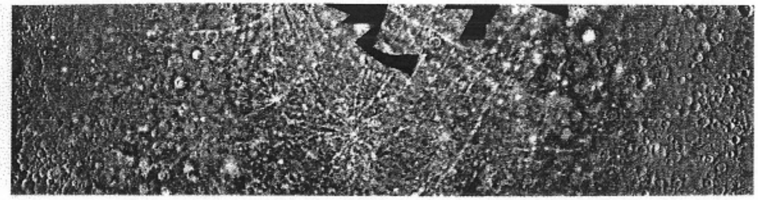

Figure 7.6. Photomosaic of the equatorial region of Mercury from about 10 to 190° longitude and ±30° latitude; the only mosaic from terminator to terminator. The photomosaic is a Mercator projection (courtesy of Jet Propulsion Laboratory).

In addition to the maps mentioned above, there are also special geologic maps of nine quadrangles. These maps are an interpretation of the geology of Mercury viewed by *Mariner 10*.

7.4 RADAR CHARACTERISTICS AND SPECIAL FEATURES

Ground-based radar observations from Arecibo, Puerto Rico, the Very Large Array (VLA) in Soccoro, New Mexico, and the Goldstone radar facility in California's Mohave Desert have contributed significantly to our knowledge of Mercury's surface. As usual, observations of Mercury are not easy. The radar disk of Mercury is comparable to a dime at 16,000 km distance! At the same time the data have been so interesting, some with multiple interpretations, that new and exciting questions have been raised.

7.4.1 Roughness, and equatorial and low latitude topography

Important radar observations of Mercury were made at the Goldstone radar facility at Fort Irwin, California in the 1970s and 1980s. At Mercury's closest approach to Earth, features down to 10 km in size could be resolved at 12.5 cm (S-band) and 3.5 cm (X-band) wavelengths. From these observations it was possible to obtain topographic profiles along equatorial regions on both the side imaged by *Mariner 10* and the unimaged side. For the terrains measured by these observations, it was found that crater rim heights were generally low and crater floor depths relatively shallow. Total topographical height differences greater than 2 km are uncommon at the spatial resolution of the radar.

Radar observations from Arecibo Observatory also measured *altimetric profiles* and identified large-scale topographic features such as subsidence zones, highlands, and smooth plains. A large, 2.5 km deep crater at 279°, 8.5°N is one of the largest structures discovered on the unimaged side.

Surface roughness and *transparency* may also be determined from radar observations. Mercury and the Moon both have average *radar cross-sections* of about 0.06 at the 13 cm wavelength. For comparison, Venus has a cross section of about 0.11, and Mars a range from about 0.04–0.15 at the 13 cm wavelength. Solid rock surfaces have cross sections of 0.15–0.25 and rock powders about 0.03–0.06. Thus, most of Mercury's surface is dominated by relatively porous regolith, rather than solid rock. This is consistent with measurements of Mercury's microwave and infrared emissions, and its photometry. Microwave observations from 0.3 to 20.5 cm indicate that Mercury's regolith is at least two to three times more transparent than the lunar maria and at least 40% more transparent than the lunar highlands. This difference is likely due to a lower abundance of iron and titanium in Mercury's regolith (see Chapter 8). Mercury's quasispecular roughness measurements (mean slopes) are very similar to the Moon's which show differences between the smooth mare surfaces (4°) and the lunar highlands (8°). These same differences are seen for Mercury's smooth plains (5.3°) and the rougher intercrater plains (8.3°). Like the Moon, there is no evidence for the extremely smooth terrain (~1°) that has been seen in some areas of Mars.

7.4.2 The Goldstein features

In 1970, two very large radar features were discovered on Mercury by Richard Goldstein of the Jet Propulsion Laboratory using the Goldstone radar facility. Circularly polarized, monochromatic waves were beamed at Mercury. Then the sense of circular polarization was reversed and more waves reflected from Mercury. The reflection from the "opposite sense" circular polarized beams revealed large radar-bright features. Two definite features were identified, with the possibility of a third. Because of north/south and spreading ambiguities inherent in the radar imaging at that time, identification of the exact location and the nature of the three radar-bright topographic features would have to wait for two decades.

The first full-disk radar imaging of Mercury was done using a direct interferometric imaging approach which does not have the north/south ambiguity of the earlier methods. The Goldstone radar facility was used to transmit the maximum signal possible to Mercury and the VLA receivers near Socorro, New Mexico were configured to receive it. By spacing the array of receivers in an optimal configuration, it was possible to obtain high spatial imaging of the surface radar reflectance at a resolution of 15 km.

One of the Goldstein features was identified with a large equatorial feature near 240°W longitude. The other Goldstein feature was resolved into two separate mid-latitude features, one in the north and one in the south. The extent of the uncertainty in the Goldstone observations became understood when it was discovered that the northern and southern features in the Goldstone/VLA image had the same longitude, close to 345°W. The three topographic features have been given the designation of radar-bright regions A (345°W longitude, −32° latitude), B (345°W longitude, 58° longitude), and C (240°W longitude, 0° latitude).

Very high-resolution (1.5–3 km) radar images at 12.6 cm wavelength obtained by the Arecibo radar facility show that both features A and B are relatively fresh impact craters with radar-bright ejecta blankets and rays. On the Moon only Tycho and Copernicus show radar-bright rays at 3.8 cm wavelength; at 70 cm wavelength they do not show at all. The radar-bright rays are probably rough ejecta and small fresh secondary impact craters that are rough at the radar wavelength of the observations. In fact, the fresh rayed craters Kuiper and Copley, seen on *Mariner 10* images, are also radar-bright. Features A and B are seen in Figure 7.7. Feature A is about 85 km diameter with an extensive ray system and a rough radar-bright floor, consistent with fresh impact crater morphology similar to Tycho or Copernicus on the Moon. Feature B is about the same size (~87 km) with radar-bright rays and a radar-dark floor. The radar-dark floor indicates it is smooth at 12.6 cm wavelength, contrary to Feature A. Feature C consists of a large circular region about 1000 km diameter consisting of small radar-bright spots. There appears to be no central structure as in Features A and B. The geologic nature of this feature is not known, but recent radar images suggest it may be a swarm of impact craters or possibly secondary impacts from an obscure crater.

7.4.3 Radar observations discover highly backscattering polar deposits

Not only did the radar imaging confirm the Goldstein features but it discovered a north polar "anomaly". There was a small area in the polar regions where a very high fraction of the incident radar was reflected back to Earth with the same characteristics as reflections from Mars' south polar cap and from the icy Galilean satellites. The signal intensity and the location suggested that Mercury had polar water ice. Follow-up observations were made with the Arecibo radar facility in Puerto Rico. While a different type of imaging was used, the results were equally interesting; not only was the north polar "anomaly" confirmed but a new south polar "anomaly" was discovered. The radar bright regions can be seen in Figure 7.7, and a map of the polar deposits is shown in Figure 7.8.

If these deposits are indeed ice, then the Moon and all terrestrial planets, except Venus, have ice deposits in their polar regions. The Greenland and Antarctic ice caps on Earth are the remnants of the last ice age that ended about 12,000 years ago. The source of the ice is, of course, Earth's oceans. The polar caps of Mars consist of both water (H_2O) and carbon dioxide (CO_2) ices. During Martian summers at the poles the CO_2 sublimes away leaving a residual cap of water ice. Recent spacecraft measurements from the *Odyssey* mission's neutron and gamma-ray spectrometer have discovered very large amounts of buried water ice down to about 60° latitude in the southern hemisphere, and in some places down to ~40° latitude in the northern hemisphere. The source of this water ice may also have been past oceans on Mars. The neutron and gamma-ray spectrometers on the *Lunar Prospector* spacecraft discovered enhanced hydrogen (H) signals in permanently shadowed craters in the polar regions of the Moon. This has been interpreted as water ice with a concentration of $1.5 \pm 0.8\%$ weight fraction.

The discovery of possible water ices at high latitudes (72°–90°N and S) in the polar regions of Mercury astounded planetary scientists and the public alike. How could this hot planet, with daylight lasting 88 Earth days and temperatures high enough to melt lead possibly have water ice at the southern and northern polar areas? More observations were taken at the same two facilities, and an upgrade

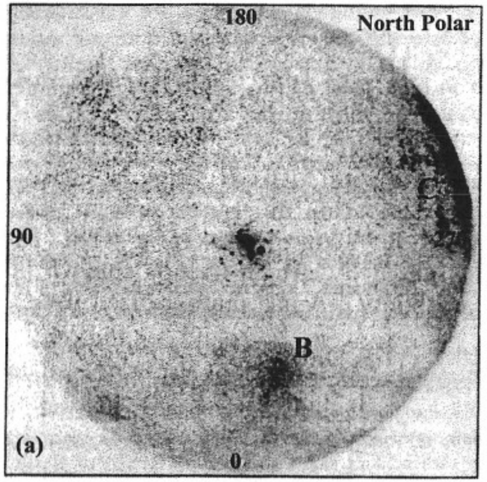

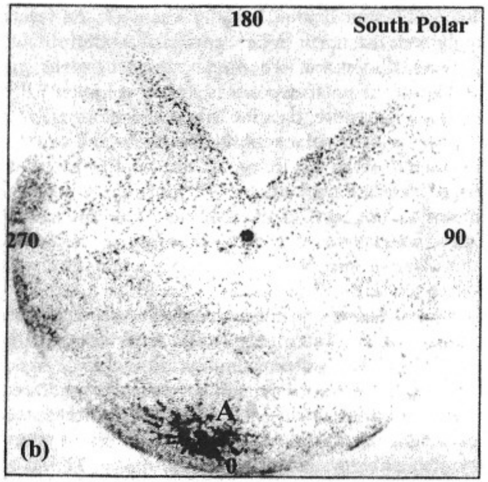

Figure 7.7. Arecibo *depolarized* radar images of the (a) northern, and (b) southern hemispheres of Mercury, in polar projection. The radar features A, B, and C are indicated on the figure. The polar deposits can also be seen near the poles (from Harmon, 1997).

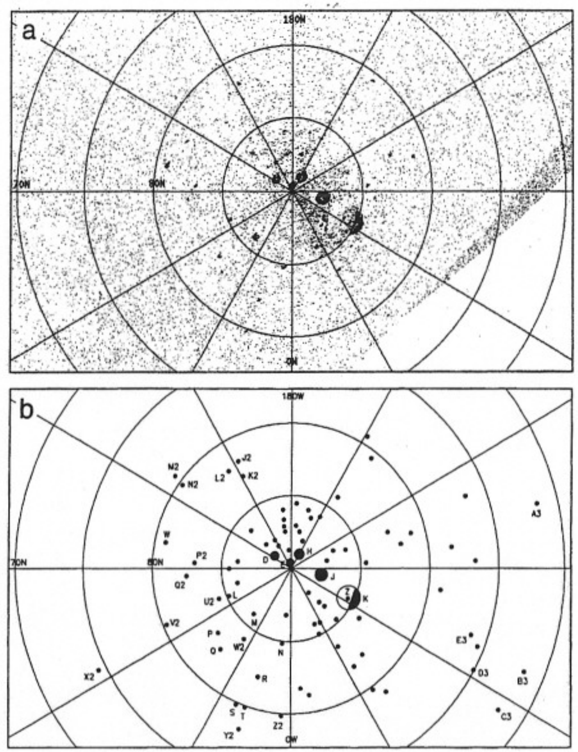

Figure 7.8. Bright radar signals from localized regions in permanently shadowed craters at high northern latitudes on Mercury's surface are shown. The actual radar image is shown in (a) with a superimposed location grid. A detailed map and numbering scheme are shown in (b) (from Harmon *et al.*, 2001).

on the Arecibo radar facility permitted even higher spatial resolution observations. Soon maps had been made of the north and south polar and high-latitude regions, that showed many locations of high radar backscatter coming from what was determined to be permanently shadowed regions in the interiors of craters. The reason Mercury has permanently shadowed craters is that its obliquity is essentially zero. Therefore, the rotation axis is perpendicular to its orbital plane around the Sun, so there are regions in craters at high-latitudes that never see the Sun. The deposits are concentrated only in the freshest craters, and even in some craters less than 10 km in diameter. Degraded craters do not show the highly radar backscattering deposits, probably because there is no permanently shadowed regions in these

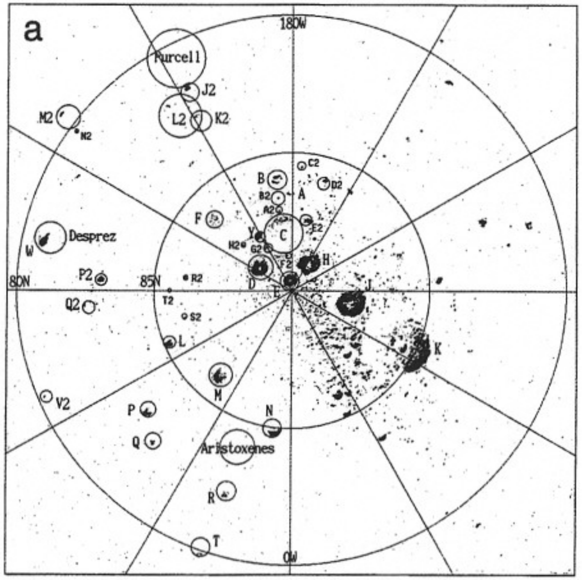

Figure 7.9. Detailed high-resolution radar image showing the radar-bright deposits in the north polar regions, and with a superposed map of their locations and designations (from Harmon *et al.*, 2001).

low-rimmed and shallow craters. In fact, the permanently shadowed cold traps are essentially full. Furthermore, the strong radar signal indicates that the material is relatively pure. The estimated thickness of the deposits is believed to be approximately between 2 and 20 m. The upper limit is, in fact, arbitrary because the radar data cannot put a upper limit on the thickness. The area covered by these deposits (both north and south) is estimated to be $\sim 3 \pm 1 \times 10^{14}$ cm^2. This would be equivalent to 4×10^{16} to 8×10^{17} g of ice, or 40–800 km^3 for a 2–20 m thick deposit. Each meter thickness of ice would be equivalent to about 10^{13} kilograms of ice.

Not only is the observational evidence strong for water ice but so are the theoretical models and calculations that have been made following the discovery. It has been calculated that water ice can be stable in the interiors of craters even down to 72° latitude if covered with only a few centimeters of dusty regolith, or if it is relatively new. This means that water ice may still linger in its perpetually shadowed craters or even in illuminated craters at high latitude if covered with a veneer of regolith. Figure 7.9 shows the actual radar image with the highly backscattering radar signals for the northern hemisphere. A map of those locations with a

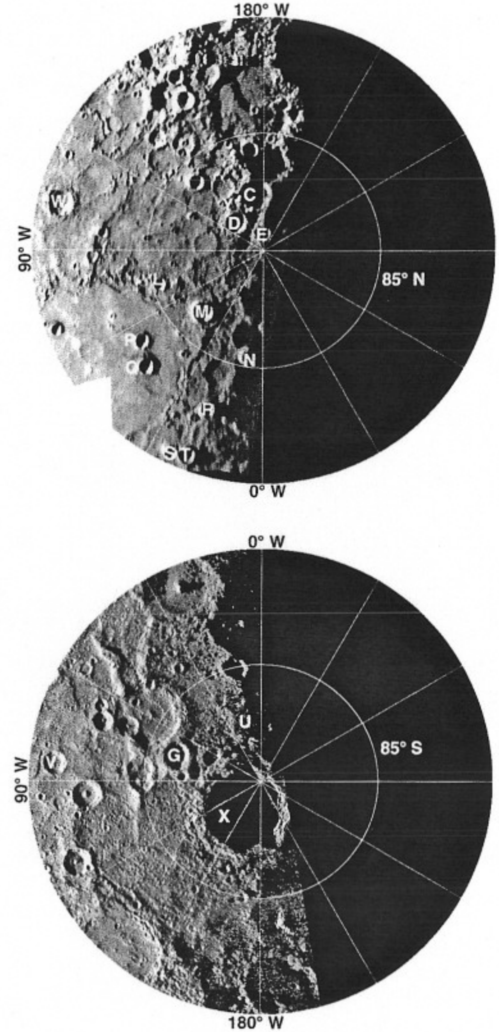

Figure 7.10. *Mariner 10* photomosaics of the north (top) and south (bottom) polar regions of Mercury showing some of the larger craters with radar bright deposits (lettered as on Figure 7.9) (courtesy Mark Robinson, Northwestern University).

numbering identification scheme is overlain on the image. Figure 7.10 includes *Mariner 10* photomosics of the north and south polar regions showing some of the larger craters with radar bright deposits.

The current evidence suggests that Mercury's polar deposits are probably water ice. The most likely sources of the water are micrometeorite, comet, and water-rich asteroid impacts. Extrapolating the current terrestrial influx of interplanetary dust particles to that at Mercury indicates that continual micrometeorite bombardment of Mercury over the last 3.5 billion years could have delivered $3–60 \times 10^{13}$ kg of water ice to the permenantly shadowed polar regions (an average thickness of 0.8–20 m). Impacts from Jupiter-family comets over the last 3.5 billion years can supply $0.1–200 \times 10^{13}$ kg of water to Mercury's polar regions (corresponding to an ice layer between 0.05–60 m thick). Halley-type comets can supply $0.2–20 \times 10^{16}$ g of water to the poles (0.1–8 m ice thickness). These sources provide more than enough water to account for the estimated volume of ice at the poles. The ice deposits could, at least in part, be relatively recent deposits, if the two radar features A and B were the result of recent cometary or water-rich asteroid impacts.

While the evidence for water ice is strong, other possibilities for the material causing the high radar backscatter signal have been suggested. Unfortunately, until this discovery there has not been much need for ground-based laboratory experiments to determine the radar properties of planetary materials. During and following World War II, there were some measurements of a variety of materials of interest to the military. Among them was sulfur (S_n, n = 2, 4, ...), a substance used as an electrical insulator. One property of a good radar backscattering material is that it is a good electrical insulator, sulfur is such a substance. A source of sulfur is the constant rain of meteoritic material. The problem with sulfur being the deposits on Mercury is that it is stable at higher temperatures than water, and there are no highly radar backscatter deposits in the polar regions where temperatures are within the stability range of sulfur. A 1-meter thick layer of water ice is stable for one billion years at a temperature of −161°C while sulfur is stable at a considerably higher temperature of −55°C. Much of the region surrounding permanently shadowed craters is less than −55°C, but there are no radar reflective deposits there. Very cold silicate glass has also been suggested as a possibility. The *MESSENGER* mission to Mercury should be able to address this problem from critical measurements made during its orbital lifetime.

8

Surface composition

8.1 ALBEDO AND COLOR

Mariner 10 made no measurements that could determine the elemental abundances, specific minerals, or rock types on Mercury. All we know about Mercury's surface composition comes from ground-based observations and inferences from color reconstructions of *Mariner 10* images. Recalibrations of the *Mariner 10* images and a technique of ratioing images and looking at relative brightness from two different colors has resulted in several important new insights into the makeup of the *regolith* and possibly its iron oxide (FeO) content. They have also suggested the location of compositional boundaries.

Albedo is one word used to quantify the percentage of light reflected back from a surface. The albedo of Mercury's surface varies from one location to another and from one wavelength to another. The human eye is sensitive to the spectral range from about 400 to 700 nm and perceives what we call the *visible spectrum*. The colors violet, indigo, blue, green, yellow, orange, and red all fall within that range. Other wavelength ranges are also referred to as having colors, just not visible colors. One way planetary surfaces are compared in their scattering and compositional characteristics is by their color. Often the color may refer to the relative albedo at one spectral region to the albedo of a different planetary surface (or atmosphere) at the same wavelength interval. The albedo of a surface will also vary when the angle of incidence and exitance of reflecting sunlight changes. Thus, to properly compare different albedo measurements, not only must the location be known but also the illumination geometry must be the same on both surfaces being compared. Thus, researchers must be careful to make comparisons that are justified within the experimental uncertainties.